JPET Fast Forward. Published on October 6, 2005 as DOI: 10.1124/jpet.105.089102

JPET #89102

Evaluation of drug penetration into the brain: a double study by *in vivo* imaging with positron emission tomography and using an *in vitro* model of the human blood-brain barrier

Véronique Josserand, Hélène Pélerin, Béatrice de Bruin, Benoît Jego, Bertrand Kuhnast, Françoise Hinnen, Frédéric Ducongé, Raphaël Boisgard, Frédéric Beuvon, Francine Chassoux, Catherine Daumas-Duport, Eric Ezan, Frédéric Dollé, Aloïse Mabondzo* and Bertrand Tavitian.

CEA, Service hospitalier Frédéric Joliot, Orsay, France: INSERM ERM 0103 (V.J., B.J., F.Du., R.B., B.T.) and radiochemistry group (B.B., B.K., F.H., F.Do.).

CEA, Service de Pharmacologie et d'Immunologie, Gif-sur-Yvette, France (H.P., E.E., A.M.)

Service de Neuropathologie, Hôpital Sainte Anne, Paris, France (F.B., C.D.)

Service de Neurochirurgie, Hôpital Sainte Anne, Paris, France (F.C.)

JPET #89102

Running Title: screening of CNS drug passage : *in vitro-in vivo* correlation

Address correspondence to: Dr. Aloïse Mabondzo, CEA, Laboratoire d'Etudes du Métabolisme des Médicaments, Service de Pharmacologie et d'Immunologie, DRM/DSV, Bâtiment 136, 91191 Gif sur Yvette Cedex, France. Phone: 33 1 69 08 13 21, Fax: 33 1 69 08 59 07. E-mail: Aloïse.Mabondzo@cea.fr

Number of text pages: 34

Number of tables: 2

Number of figures: 8

Number of references: 40

Number of words in the abstract: 248

Number of words in the introduction section: 831

Number of words in the discussion section: 1543

List of nonstandard abbreviations:

PET: positron emission tomography

BCRP: breast cancer resistance protein

MRP: multi-drug-resistance protein

IDM: indicator diffusion method

HPLC: high pressure liquid chromatography

PBS: phosphate buffered saline

Recommended section assignment: Neuropharmacology

ABSTRACT

The blood brain barrier (BBB) permeabilities of 11 compounds were measured both *in vitro* with a newly developed co-culture based model of human BBB, and *in vivo* with positron emission tomography (PET). The 11 compounds were fluoropyridinyl derivatives labeled with the positron-emitter fluorine-18 : [^{18}F]F-A-85380 (2-[^{18}F]fluoro-3-[2(S)-2 azetidinylmethoxy]pyridine and 10 selected *N*-substituted-azetidinyl and pyrrolidinyl closely-related [^{18}F]fluoropyridinyl derivatives (including [*N'*-aromatic/aliphatic]-thioureas, -ureas, and -amides). The *in vitro* BBB model, a new co-culture system of primary human brain endothelial cells and astrocytes, was used to measure the permeability coefficient for each compound. Dynamic PET studies were performed in rats with the same compounds and a two-compartment model analysis was used to calculate their *in vivo* permeability coefficients. The 11 derivatives differed in their degree of BBB passage and transport mechanism. The analysis of PET data showed a significant cerebral uptake for six derivatives, for which the *in vitro* evaluation indicated active influx or free diffusion. Five derivatives displayed low *in vivo* cerebral uptake, in agreement with the observation of an *in vitro* active efflux. Overall there was a remarkable correlation between the *in vitro* and *in vivo* permeability coefficients ($r = 0.99$). This double study evidences a close correlationship between the assessment of the BBB passage *in vitro* and *in vivo*. The *in vitro* model of human BBB offers the possibility of subtle discrimination of various BBB permeability degrees and transport mechanisms. Conversely, small animal PET imaging appears suitable to screen, directly *in vivo*, drugs or radiopharmaceuticals candidates aimed at cerebral targets.

INTRODUCTION

In mammals, the presence of tight junctions connecting the endothelial cells of the brain vessels creates a blood-brain barrier (BBB) that limits to a considerable extent the delivery of systemically administered drugs to the central nervous system (CNS). In addition, specific metabolizing enzymes and efflux pumps located within the endothelial cells actively degrade or reject exogenous molecules out of the brain (Schinkel et al., 1994; Huai-Yun et al., 1998; el-Bacha and Minn, 1999; Bendayan et al., 2002).

As a consequence, the development of drugs targeting the CNS requires a precise knowledge of their brain penetration and, ideally, this information should be obtained as early as possible. This is a major challenge for the design of CNS drugs since (i) prediction of BBB passage from the chemical structures is largely unreliable and (ii) as far as concerned with new compounds for which toxicological knowledge is lacking, it is not possible to test drug penetration directly in Humans *in vivo*. Hence, testing the brain passage of drug candidates of pharmaceutical importance for CNS diseases relies on surrogate estimates of blood-to-brain passage established on *in vitro* and *in vivo* models of the BBB.

In vitro models are based on the reconstitution of the BBB by cell cultures of non cerebral peripheral endothelial cell lines, immortalized rat brain endothelial cells (Begley et al., 1996), primary cultured bovine, porcine or rat brain capillary endothelial cells (Audus and Borchardt, 1986; Van Bree et al., 1988; Hughes and Lantos, 1989; Weber et al., 1993; Franke et al., 1999), and of co-cultures of primary brain capillary cells with astrocytes or astrocyte-conditioned medium (Dehouck et al., 1992; Pardridge et al., 1990; Rubin et al., 1991; Gaillard et al., 2001; Mégard et al., 2002; Jeliazkova-Mecheva and Bobilya, 2003; Parkinson et al., 2003). Co-culture systems produce monolayers with tight junctions joining the endothelial cells, in which the polarity of transport can be evaluated by measuring the passage from apical

to basolateral surface or *vice versa*. Whatever their ressemblance with the BBB, *in vitro* models must be carefully assessed for their capacity to describe accurately the passage of drugs into the CNS *in vivo*.

Alternatively, several *in vivo* experimental setups have been used to estimate the BBB passage of drugs directly in laboratory animals. *In vivo* transport across the BBB was first studied in the 1960s using the early indicator diffusion method (Crone, 1963). Other *in vivo* techniques were later proposed: brain uptake index (BUI) measurement (Oldendorf, 1970), *in situ* brain perfusion or brain efflux index methods (Takasato et al., 1984; Kakee et al., 1996), autoradiography and intracerebral microdialysis (Elmquist and Sawchuk, 1997). Although they require various levels of equipment, technical expertise and mathematic modeling, all these *in vivo* methods have important limitations, notably their invasiveness which may lead to non physiological BBB passage. In contrast, functional imaging with Positron Emission Tomography (PET) is a non invasive imaging technique increasingly used in drug discovery (Gupta et al., 2002; Wong and Pomper, 2003; Laruelle et al., 2003) and it has been demonstrated to be applicable to the non invasive measurement of BUI in baboons (Dishino et al., 1983). PET is today the most advanced technology to obtain biochemical information such as glucose metabolism, blood flow, and distribution of receptors, enzymes and neurotransmitters, directly *in vivo*, because it is non invasive, rapid and repeatable and offers very high sensitivity. Thus, it allows monitoring of the whole pharmacokinetic time-course in physiological conditions on the same animal. Brain kinetics can be analyzed by compartmental modeling which allows the calculation of the relevant rate constants that describe the BBB passage (Koeppe et al., 1990; Wiesel et al., 1991; Hendrikse et al., 2001).

Up to date, all models, whether *in vitro* or *in vivo*, remain mere approximates of the complex Human BBB and their relevance to the real life situation must be carefully controlled. An interesting way to do so is to cross-compare the BBB passage of a series of compounds

evaluated with both *in vitro* and *in vivo* models alongside each other. This enables cross-correlations of the *in vitro* and *in vivo* pharmacokinetic data and the assessment of the predictive power of both tests.

The present work reports for the first time the evaluation of the BBB permeabilities of a series of compounds studied correlatively *in vitro* using a new Human BBB co-culture system and *in vivo* with quantitative PET imaging in rats. The tested compounds are 11 selected fluorine-18-labeled fluoropyridinyl derivatives including (a) the radiopharmaceutical [^{18}F]F-A-85380, (2-[^{18}F]fluoro-3-[2(S)-2-azetidinylmethoxy] pyridine) a selective and high-affinity radioligand which is currently used for the study of the $\alpha_4\beta_2$ nicotinic acetylcholine receptors in the human brain with PET (Dollé et al., 1998; Dollé et al., 1999; Kimes et al., 2003; Bottlaender et al., 2003) and (b) 10 selected *N*-substituted-azetidinyl and -pyrrolidinyl closely-related [^{18}F]fluoropyridinyl derivatives (including [*N'*-aromatic/aliphatic]-thioureas, -ureas, and -amides) named [^{18}F]FPy 01 to 10. Comparative measurements of the BBB passage of the complete series of compounds, estimated from the *in vitro* Human BBB model and from the *in vivo* PET technique, are discussed.

METHODS

Labeled derivatives

[^{18}F]F-A-85380 (2-[^{18}F]fluoro-3-[2(S)-2-azetidinylmethoxy]pyridine) was prepared as previously described (Dollé et al., 1999). Briefly, [^{18}F]F-A-85380 was synthesized by no-carrier-added nucleophilic aromatic substitution by K[^{18}F]F-K_{222} complex with (3-[2(S)-*N*-(tert-butoxycarbonyl)-2-azetidinylmethoxy]pyridin-2-yl)trimethylammonium trifluoromethanesulfonate as a highly efficient labeling precursor, followed by TFA removal of the Boc protective group and HPLC purification (total synthesis time : 50-53 min from the end of cyclotron fluorine-18 production; radiochemical yields, with respect to initial [^{18}F]fluoride ion radioactivity : 68-72% (decay-corrected) and 49-52% (non-decay-corrected); specific radioactivities at the end of the synthesis: 2-5 Ci/µmol (74-185GBq/µmol).

The 10 selected *N*-substituted-azetidinyl and -pyrrolidinyl closely-related [^{18}F]fluoropyridinyl derivatives, named [18F]FPy 01 to 10 **(figure 1),** were prepared using a similar chemical approach to the one described above for the preparation of [^{18}F]F-A-85380, followed by (1) condensation reaction of the cyclic amine with the appropriate commercially available isothiocyanate, isocyanate or acylhalide and (2) final HPLC purification to give the expected corresponding *N*-aromatic/aliphatic]-thioureas, -ureas, and -amides.

Measurement of octanol: phosphate saline buffer partition coefficient

500 µL of octanol were added to each fluorine-18-labeled fluoropyridinyl derivatives (3700 kBq) diluted in 500 µL of PBS (Dulbecco's Phosphate Buffered Saline, Life Technologies, pH 7.4).

The vial was shaken for 3 min and the resulting homogenate was centrifuged for 5 min at room temperature. An aliquot (100 μL) of each phase was counted for radioactivity in a calibrated γ-counter (Cobra Quantum, Packard).

In vitro human BBB model

The BBB model was a co-culture of primary human brain endothelial cells (BECs) and primary human astrocytes (HA) as previously described (Mégard et al., 2002). The isolation of these cells was essentially based on the methods described by Deli and colleagues (Deli and Joo, 1996). Immunocytochemistry specific for the HA and the BECs was conducted in order to check the purity of the cultures. BECs were washed twice with PBS and incubated during 3 h at 37°C with 1-methyl-[^{14}C]-1,1'-dioctadecyl-3,3,3',3'-tetramethylindocarbocyanine perchlorate acetylated low-density lipoprotein (DiI-acyl-LDL) (10 μg.mL^{-1}) (Sigma, St Louis, MO), then washed three times with PBS and fixed with paraformaldehyde (PFA) in PBS as previously described (Mégard et al., 2002). Moreover, BECs or Astrocytes were fixed in PBS, 4% PFA and were incubated in PBS, 0.1% Triton X-100 for 10 min at room temperature. Cells were then washed in 5% bovine serum albumin (BSA) for 30 min at room temperature, rinsed twice with PBS and stained with mouse mAb (IgG1) against CD31 (for BECs), against GFAP (for astrocytes) or with the isotypic mouse IgG1 mAb (Becton-Dickinson, San Diego, CA) as reported previously (Mégard et al., 2002). BEC monolayers grown on the filter were fixed with cytofix-cytoperm buffer (Pharmigen, France) and permeabilized with Perm/Wash buffer (Pharmigen) according to the manufacturer's procedure. The samples were washed with PBS and soaked in the blocking solution containing 4% BSA. They were then incubated with the mouse anti-claudin-5 mAb (Zymed laboratories, San Francisco, CA). After specific washes, the cells were incubated with

JPET Fast Forward. Published on October 6, 2005 as DOI: 10.1124/jpet.105.089102
This article has not been copyedited and formatted. The final version may differ from this version.

the secondary Ab Alexa fluor 488 goat anti-mouse IgG. The preparations were examined with confocal fluorescence microscopy.

Briefly, to obtain the co-cultures, HA (5 x 10^4 cells) were plated on transwell plates (Costar, Dutscher sa, Brumath, France) in an astrocyte-specific basal medium (α-MEM, DMEM, suplemented with 10 µg mL^{-1} hEGF, 10 mg ml^{-1} insulin, 25 µg ml^{-1} progesterone, 50 mg ml^{-1} transferrin, 50 mg ml^{-1} gentamicin, 50 µg mL^{-1} amphotericin-B and 5% FBS). The medium was removed twice a week.

After 72 h, BECs (5 x 10^4 cells) were seeded on the upper side of a collagen-coated polyester TranswellR membrane (Costar, pore size 0.4 µm; diameter 12 mm; insert growth area 1 cm^2) in the BECs-specific medium (0.5 mL). The chambers containing the HA and the BECs were considered as the basal and the apical compartments, respectively. The microplates were then incubated at 37°C in a 5% CO_2 atmosphere. Under these experimental conditions, BECs formed a confluent monolayer within 15-20 days (Mégard et al., 2002).

Before the *in vitro* human BBB model was used to measure the BBB passage of the [^{18}F]fluoropyridinyl derivatives, the integrity of the BBB monolayer was estimated by measuring on three wells the flux through the monolayer of the paracellular reference marker [^{14}C]sucrose (12.95 MBq.µmol^{-1}) (Amersham Buckinghamshire, UK) as described previously (Mégard et al., 2002).

In vitro drug transport study

Just before the transport experiments, the astrocytes were removed from the basal compartment and the medium from both apical and basal compartments were replaced by brain microvascular endothelial cell-specific medium and astrocyte-specific medium respectively.

JPET Fast Forward. Published on October 6, 2005 as DOI: 10.1124/jpet.105.089102
This article has not been copyedited and formatted. The final version may differ from this version.

Experiments were made in triplicate for each fluoropyridinyl derivatives. The radiolabeled compound (185 kBq) was introduced in the donor chamber (either the apical or the basal compartment). At various time points (5; 10; 15; 20; 30 and 40 min) after the addition of the radiolabeled compound, aliquots of the medium were removed from the acceptor chamber (basal or apical compartments respectively) for radioactivity counting and were replaced by fresh medium.

Data analysis

Permeability calculations were performed as described by Pardridge et al. (1990). The fraction of radioactivity transported from the donor to the acceptor chamber at each time point was multiplied by the volume of the donor chamber, to give the equivalent volume cleared at a given time point. The volume cleared was plotted versus time (clearance curve) and analyzed by linear regression. The clearance curve was linear up to 40 min for all derivatives. The slope of the clearance is the permeability coefficient PS expressed in $\mu L.min^{-1}$, where P is the permeability in $mm.min^{-1}$ and S the filter area in mm^2).

PS was measured both from the wells containing the filter plus endothelial cells (PStot) and from the wells with filter alone (PSf).

The PS value strictly due to the endothelial monolayer is called PSe and was calculated as follows:

$1/PSe = 1/PStot - 1/PSf$ (1)

$PSe = (PSf \times PStot) / (PSf - PStot)$ (2)

PSe was measured both from the apical to basal compartment (PSe-in) and from the basal to apical compartment (PSe-out) and the PSe-out / PSe-in ratio (Q ratio) was calculated.

***In vivo* PET imaging**

All animal experiments were conducted in agreement with the "Principles of laboratory animal care" (NIH publication No. 86-23, revised 1985). Male Wistar rats (200-250 g, IFFA Credo, France) were anaesthetized (isoflurane/oxygen 5% for induction and 3% thereafter) and catheterized in the tail vein. A transmission scan with a Germanium-68 source was done for attenuation correction. The [^{18}F]fluoropyridinyl derivative (14.8-15.5 MBq) was intravenously injected simultaneously into four anesthetized rats and PET imaging was performed during 60 min with the EXACT HR+ camera (Siemens) with increasing time frames, starting with 24 frames of 10 s, followed by 18 frames of 20 s, 20 frames of 30 s and finally 40 frames of 60 s.

The raw data were reconstructed using an Ordered Subset Expectation Maximization Weighted Attenuation (OSEM-WA) with 6 iterations and 8 subsets including a Fourier rebinning.

To determine the pharmacokinetics of the [^{18}F]fluoropyridinyl derivatives in the brain, cerebral PET images were analyzed by drawing volumes of interest (VOI) on the brain area visualized on 8 consecutive sections encomparing the complete brain volume of the animals. For comparison, all values of radioactivity concentrations were normalized by the injected dose, and expressed as percentage of the injected dose per volume of tissue (%ID.cm^{-3}).

Arterial kinetics and métabolism

In order to estimate the input function, 14.8-15.5 MBq (200-250 μL) of each [^{18}F]fluoropyridinyl derivative were injected to two animals. Arterial blood samples (20 to 30 ul) were removed at 1, 3, 6, 9, 12, 15 s, then every 5 s up to 2 min and finally every 10 min until 1 h post-injection. Whole blood radioactivity was measured in a calibrated γ-counter (COBRA II, Packard).

JPET Fast Forward. Published on October 6, 2005 as DOI: 10.1124/jpet.105.089102
This article has not been copyedited and formatted. The final version may differ from this version.

In order to estimate the metabolism, 26.2-30.6 MBq (200-250 µL) of each [^{18}F]fluoropyridinyl derivative were injected to a rat and 1 mL of arterial blood was removed at 5 minutes post injection. RadioHPLC was used to measure the proportion of the intact compound in plasma.

***In vivo* data analysis**

The whole blood kinetics and the brain kinetics obtained from PET data were analyzed according to a two compartment-model **(figure 2)**.

The operational equation of this model was:

$dCb(t)/dt = k1.Ca(t) – k2.Cb(t)$ (3)

where k1 is the influx rate constant expressed in milliliter of blood per cubic centimeter of tissue per minute ($mL.cm^{-3}.min^{-1}$), k2 the efflux rate constant (min^{-1}), Cb(t) the concentration of radioactivity in the brain and Ca(t) the arterial input function.

The biomedical software PMOD (PMOD technologies, Zurich, Switzerland) was used to calculate the pharmacokinetic parameters k1, k2 from each individual experimental arterial kinetic data ($kBq.mL^{-1}$) and the average brain kinetic data ($kBq.cm^{-3}$). The fit quality is estimated by the software and is reflected by the variation coefficients on k1 and k2 (table 2). The distribution volume (DV) is the ratio k1/k2 expressed in milliliter of blood per cubic centimeter of tissue ($mL.cm^{-3}$). These calculations take into account the cerebrovascular blood volume which was approximated to be 0,1 mL for the rat.

k1 reflects the rate of drug absorption into the brain, also called clearance of the drug.

$k1 = Q \times E$ (4)

where Q is the blood flow ($mL.min^{-1}$) and E is the extraction ratio, a unitless quantity reflecting the proportion of drug removed from blood across the BBB.The extraction ratio E of a drug as it moves through the capillary bed can be described by an exponential equation

involving the permeability coefficient of the drug corrected for the area of the capillary bed and for the flow rate through the bed.

$$E = 1 - \exp^{(-PS/Q)} \qquad (5)$$

where PS is the permeability x surface area product expressed in milliliter of blood per minute per cubic centimeter of tissue ($mL.min^{-1}.cm^{-3}$), P is the permeability coefficient expressed in $cm.min^{-1}$ and S is the total area of the capillary bed expressed in square centimeters of capillary per cubic centimeter of tissue ($cm^2.cm^{-3}$).

From (4) and (5):

$$k1 = Q\,(1 - \exp^{(-PS/Q)}) \qquad (6)$$

Hence, PS can be deduced from equation (6):

$$PS = -Q \times Ln\,(1 - k1/Q) \qquad (7)$$

Q was approximated to be to be 1.3 $mL.min^{-1}$ as previously published (Davies and Morris., 1993).

***In vitro-in vivo* correlation study**

When attempting to measure drug transport across the BBB, beyond the choice of the most relevant experimental models, it is essential to determine which *in vitro* and *in vivo* parameters are (i) the most significant and (ii) can be used for comparison in the respective models. The present study focused on the transport stage without taking into consideration the fate of compounds once they have entered the brain. Using a two-compartment model to calculate the pharmacokinetic parameters of the BBB passage *in vivo*, (i.e. the influx rate constant k1 and the efflux rate constant k2) allowed a direct comparison of the clearance of the compound from blood to brain ($ml/min/cm^3$ of tissue), the same parameter being measured in the co-culture based model from the apical to the basal compartment (µl/min).

The *in vitro* PSe-in and the *in vivo* PS were both calculated from their respective measured clearances so the comparison of these two parameters should be very accurate.

Statistical Analysis

Statistical analysis was performed using the Prism 3.0 program (GraphPad Software, Inc, San Diego, CA). Regression lines were calculated and correlation was estimated by the two-tailed non-parametric Spearman test.

JPET Fast Forward. Published on October 6, 2005 as DOI: 10.1124/jpet.105.089102
This article has not been copyedited and formatted. The final version may differ from this version.

RESULTS

In vitro human BBB model

Specific immunocytochemical labeling with anti-GFAP mAb on astrocytes and di-I-acyl-LDL uptake in BECs or Becs stained for CD31 are illustrated in **figures 3A, 3B and 3C** respectively. In the co-culture model, BECs formed a confluent monolayer within 15 days. **Figure 3D** shows the continuous network of labeled claudin-5 demonstrating that the co-cultured endothelial monolayer displayed well developed tight junctions in the *in vitro* human BBB model.

In vitro drug transport study

Before the *in vitro* human BBB model was used to measure the BBB passage of the [^{18}F]fluoropyridinyl derivatives, the tightness of the BEC monolayer was checked by assessing the permeability of [^{14}C]sucrose. The very low permeability coefficient measured for [^{14}C]sucrose (PSe-in = 1.0 ± 0.15 $\mu L.min^{-1}$) demonstrated the integrity of the BECs monolayer. The permeability of the [^{18}F]fluoropyridinyl derivatives was then measured on the ways in and out (PSe-in and PSe-out) and the PSe-out/PSe-in ratio (Q ratio) was calculated **(table 1)**.

The *in vitro* model allows the assessment of the BBB permeability of the drug in both directions (influx and efflux) independently. Compounds which display efflux at least twice that of the influx (Q ratio above 2) are considered to undergo an effective efflux and compounds which display efflux less than or equal to the influx (Q ratio below or close to 1.0) are considered to undergo an effective influx or a free diffusion, respectively. Effective efflux and influx imply the involvment of an active transporter.

JPET Fast Forward. Published on October 6, 2005 as DOI: 10.1124/jpet.105.089102
This article has not been copyedited and formatted. The final version may differ from this version.

In this study, the Q ratio ranged from 0.5 to 4.0. Four derivatives ([^{18}F]FPy 01, 03, 07, 09) showed a Q ratio below 0.8 suggesting that these compounds cross the BBB by active transport. Two derivatives displayed a Q ratio close to 1 ([^{18}F]F-A-85380 and [^{18}F]FPy 08) suggesting that these compounds cross the BBB by free diffusion. Five derivatives showed a Q ratio above 2.0 ([^{18}F]FPy 02, 04, 05, 06, 10) suggesting that these compounds are subject to active efflux.

Octanol/phosphate saline buffer (pH 7.4) partition coefficients (log D) were measured for each derivative. Neither the molecular weights nor the log D correlated with the *in vitro* permeability coefficients (r^2 = 0.054 and 0.068 respectively).

***In vivo* studies**

The metabolism analysis showed that all compounds were essentially intact in blood 5 minutes after injection (intact compound ≥ 98 % of total blood radioactivity).

Whole body PET images acquired over 2 min after the intravenous injections of the radiolabeled molecules are shown in **figure 4**. At this early time-point, high activity in the brain was clearly seen for derivatives [^{18}F]FPy 01, 03, 08, 09 and 10 and low activity was evidenced for derivatives [^{18}F]F-A-85380, [^{18}F]FPy 02, 05, and 06.

Figure 5 shows the percentage of the injected dose taken up per cm^3 of brain (%ID.cm^{-3}) from 10 s to 3 min after the i.v. injection. The parent compound [^{18}F]F-A-85380 showed an early and fugacious peak of 0.26 ± 0.02 %ID.cm^{-3}, at 20 s after i.v. injection, after which the cerebral uptake gradually increased to a plateau reached at 40 min post-injection (0.5 ± 0.03 %ID.cm^{-3}). These findings are in agreement with the binding of this compound to the cerebral $\alpha_4\beta_2$ nicotinic receptors and with reported biodistribution studies in rodents (Dollé et al., 1999). In contrast, the derivatives peaked between 0.4 and 1.8 %ID.cm^{-3} in a time range of 20

JPET Fast Forward. Published on October 6, 2005 as DOI: 10.1124/jpet.105.089102
This article has not been copyedited and formatted. The final version may differ from this version.

s to 50 s, after which all derivatives showed a decrease in their brain activity up to 60 min, reflecting the lack of cerebral accumulation.

The pharmacokinetics of the BBB passage were analyzed according to a two compartment-model (arterial blood and brain tissue), separated by the BBB. The *in vivo* cerebral and whole blood kinetics (**figures 5 and 6**) were analyzed according to this model and the influx rate constant (k1), the efflux rate constant (k2), the distribution volume (DV) and the permeability coefficient (PS) were calculated **(table 2).** k1 and k2 ranged from 0.10 to 2.00 $mL.cm^{-3}.min^{-1}$ and from 0.04 to 2.08 min^{-1} respectively. [^{18}F]F-A-85380 displayed the smallest values for k1 and k2 (0.10 $mL.cm^{-3}.min^{-1}$ ± 2.4% and 0.04 min^{-1} ± 4%) indicating a very slow entry and an even slower efflux. These results are in agreement with the binding of this compound to the cerebral $\alpha_4\beta_2$ nicotinic receptors, which restricts the efflux, and with previous PET studies in baboons and humans (Valette et al., 1999; Kimes et al., 2003; Bottlaender et al., 2003).

In vivo **versus** ***in vitro*** **studies**

[^{18}F]F-A-85380 displayed an in vitro Q ratio close to 1 (Q = 0.9), indicating a free diffusion into the brain by passive influx while in vivo, the PET analysis demonstrated a gradual cerebral uptake (DV = 2.33) which reached a plateau at 40 min post-injection. Those results indicated that [^{18}F]F-A-85380 enters the brain by a passive influx and is not subject to efflux out of the brain..

When comparing the *in vitro* PSe-out/PSe-in ratio (Q ratio) with the *in vivo* distribution volume (DV) **(figure 7)** the compounds segragated in two groups : derivatives with an *in vitro* Q ratio above 2.0 (active efflux) displayed low *in vivo* DV (below 0.6), corresponding to a slight cerebral entry ([^{18}F]FPy 02; 04; 05; 06; 10). Conversely, derivatives with an *in vitro* Q close to or below 1.0 (free diffusion or active influx, respectively) displayed high *in vivo* DV (above 0.6) reflecting their cerebral penetration ([^{18}F]F-A-85380; [^{18}F]FPy 01; 03; 07; 08; 09).

JPET Fast Forward. Published on October 6, 2005 as DOI: 10.1124/jpet.105.089102
This article has not been copyedited and formatted. The final version may differ from this version.

Moreover, the *in vitro* permeability coefficient PSe-in determined with the *in vitro* human BBB model showed a highly significant correlation with the *in vivo* permeability coefficient (PS) calculated from the *in vivo* cerebral and plasma kinetics ($r^2 = 0.985$; $p < 0.001$; **figure 8)**.

JPET Fast Forward. Published on October 6, 2005 as DOI: 10.1124/jpet.105.089102
This article has not been copyedited and formatted. The final version may differ from this version.

DISCUSSION

Physico-chemical characteristics of drugs, such as molecular size and weight, lipophilicity, affinity and selectivity for the target site, or the metabolic profile, are generally inadequate to predict with accuracy their passage through the Human BBB (Tanaka and Mizojiri, 1999; Wong and Pomper, 2003; Laruelle et al., 2003). This was confirmed in the present study in which the tested compounds were in a relatively narrow range of molecular weights (266.3 to 585.6 $g.mol^{-1}$) and lipophilicities (log D, 0.63 to 1.95). Neither of these characteristics correlated with the measured permeability coefficients (r^2 = 0.054 and 0.068 respectively), nor was any relationship found between the biochemical structure and the BBB permeability. These results highlight the necessity to screen compounds intended to target the brain beyond their biochemical characteristics, and to actually assess their permeability across the BBB either *in vitro* or *in vivo.*

In vitro models of the BBB have the advantage to be based on cell cultures that are relatively easy to implement and standardize and avoid the use of animals. However, a major factor that may restrict brain uptake is the presence of efflux pumps within the endothelial cells, such as the P-glycoprotein (P-gp), the breast cancer resistance protein (BCRP) and the multi-drug-resistance protein (MRP) which act to keep non-essential molecules out of the brain (Schinkel et al., 1994 ; el-Bacha and Minn, 1999; Bendayan et al., 2002). Among the many *in vitro* models described, only a few have demonstrated the presence and functionality of these efflux transporters (Bendayan et al., 2002). In addition, except for the recently published porcine and rat models (Jeliazkova-Mecheva and Bobilya, 2003; Parkinson et al., 2003), most co-culture based models display interspecies or age differences between the two cell types. This may not be relevant to achieve correct function, since brain uptake may be restricted by the activity,

within the cerebrovascular endothelial cells, of several families of metabolizing enzymes which are known to be species-specific (el-Bacha and Minn, 1999).

The new co-culture based model of Human BBB presented here consists of primary cultures of Human brain capillary endothelial cells, co-cultivated with primary cultures of Human astrocytes (Mégard et al., 2002). It is worth noting that this is the first establishment of a Human astrocyte/endothelial cell co-culture BBB model. The advantages of this system are that (i) it is made of primary culture cells, (ii) it avoids species, age and inter-individual differences since the two cell types are removed from the same person, (iii) it has been shown to express functional efflux transporters such as P-gp (Mégard et al., 2002), MRP-1 and BCRP (data not shown).

Direct *in vivo* evaluation of drug passage of the BBB is ideal, but, as far as concerned with new compounds for which toxicological knowledge is lacking, it is limited to laboratory animals. Rodent models provide the best first guess provided that species differences are accounted for when necessary. This raises the issue of the relevance of animal BBB to Human BBB. In this respect, even though species differences in metabolizing enzymes exist (Schellens et al., 2000), various rat membrane bound transporters, among which P-gp, have been demonstrated to have a strong homology with the human proteins (Schinkel et al., 1994). Moreover, recent progresses in molecular imaging techniques now allow the assessment of drug distribution *in vivo* non invasively. This is particularly the case with PET, a whole body imaging technique that can measure quantitatively in real time the tissular distribution of positron-emitter labeled compounds. Progress in spatial resolution and in labeling techniques now permit dynamic quantitative measurements of drug pharmacokinetics in the organs of small laboratory animals.

Whether *in vitro* or *in vivo*, the validity of models pretending to describe such a complex system as the BBB must be tested with a series of compounds with different BBB

JPET Fast Forward. Published on October 6, 2005 as DOI: 10.1124/jpet.105.089102
This article has not been copyedited and formatted. The final version may differ from this version.

permeabilities. It is classical, in situations in which a physiological mechanism is not directly measureable, to compare the results obtained by two models in a series of independent measurements. In particular, the prime importance of cross-correlating *in vitro* and *in vivo* pharmacokinetic data, in order to validate experimental models and to assess the predictive power of the techniques, has long been recognized. Accordingly, several studies have conducted *in vitro* and *in vivo* BBB transport evaluations alongside each other (Pardridge et al., 1990; Dehouck et al., 1992; Pirro et al., 1994; Friebe et al., 2000; Lundquist et al., 2002). An in *vitro/in vivo* correlation study using another imaging technique has been previously published (Pirro et al., 1994). The BBB permeability was evaluated with both an *in vitro* bovine BBB model and the *in vivo* single-pass brain extraction measured by SPECT. Despite a good preliminary *in vitro/in vivo* correlation for seven compounds, the authors found that several 99mTc complexes displayed no concordance between *in vitro* permeability indices and *in vivo* single-pass cerebral extraction. Pardridge et al. (1990) compared an *in vitro* BBB model consisting of bovine brain capillary endothelial cell monolayer and the internal carotid artery perfusion/capillary depletion *in vivo* method. The study demonstrated a correlation between the *in vitro* and *in vivo* Ln permeability x surface area products ($r = 0.85$). However, overestimation of PSe values for lipid-mediated transport and underestimation of PSe values for carrier-mediated transport were observed with this *in vitro* model. These findings were attributed to the loss of expression of BBB-specific proteins in endothelium cultured in the absence of astrocytic trophic factors, which are normally secreted owing to the close apposition of astrocytes on brain capillary endothelial cells *in vivo* (DeBault et al., 1980). To thwart this problem, the co-culture of brain capillary endothelial cells and astrocytes was pioneered by Dehouck *et al* in 1990 and it was compared with the intracarotid injection *in vivo* method. The results showed a correlation ($r = 0.88$) between the *in vitro* and *in vivo* brain extraction values (Dehouck et al., 1992). The same group demonstrated the superiority of the

co-culture system by comparing the *in vivo* brain extraction using the Oldendorf method and the *in vitro* permeability coefficient measured either with a primary culture of brain microvessel endothelial cells or with a co-culture of brain capillary endothelial cells and astrocytes. In both cases the *in vivo* and *in vitr*o permeability values correlated but the co-culture based model displayed better indications than the endothelial cells monolayer (r = 0.90 and 0.96 respectively).

This strategy was followed in the present study, in which the BBB passage of a series of compounds was evaluated with both *in vitro* and *in vivo* models alongside each other, enabling cross-correlations of the *in vitro* and *in vivo* pharmacokinetic data and the assessment of the predictive power of both tests. The present work reports for the first time the evaluation of the BBB permeabilities of a series of compounds, studied correlatively *in vitro* using a Human BBB co-culture system, and *in vivo* with whole body PET scanning in rats. This study intended to evaluate if the *in vitro* BBB model and the *in vivo* PET method could be able to evidence any BBB passage differences related to small chemical structures variations.

The 11 tested derivatives differed in their degree of BBB passage and transport mechanism and we cast new light on the close relationship between the *in vitro* and *in vivo* pharmacokinetic data. Two major observations should be pointed out : Firstly, an *in vitro/in vivo* correlation was found between the *in vitro* Q ratio and the *in vivo* DV, allowing the discrimination between two groups of compounds: five derivatives ([^{18}F]FPy 02; 04; 05; 06; 10) displayed low or absent *in vivo* cerebral penetration (DV < 0.6), in agreement with an active efflux observed *in vitro* (Q > 2). Conversely, for six derivatives ([^{18}F]F-A-85380; [^{18}F]FPy 01; 03; 07; 08; 09) for which the PET analysis demonstrated a cerebral uptake (DV > 0.6), the *in vitro* evaluation indicated either free diffusion (Q ~ 1) ([^{18}F]F-A-85380, [^{18}F]FPy

JPET Fast Forward. Published on October 6, 2005 as DOI: 10.1124/jpet.105.089102
This article has not been copyedited and formatted. The final version may differ from this version.

08) or active influx (Q < 1) ([^{18}F]FPy 01; 03; 07, 09). Secondly, we established a strong correlation between the *in vitro* and *in vivo* permeability coefficients (r = 0.99).

Interestingly, the *in vitro* BBB model provides additional pharmacological information with regard to the *in vivo* evaluation. Indeed, the compounds with low *in vitro* Pse-in ([^{18}F]F-A-85380; [^{18}F]FPy 10, 05) can't be well separated on the *in vivo* scale since their *in vivo* PS are close to zero (0.10; 0.15 and 0.16 respectively). This may result from the restricted sensibility of the *in vivo* method for the discrimination of low entry capacity compounds in comparison with the very subtle *in vitro* evaluation. Furthermore, while *in vivo* cerebral pharmacokinetics supply global information on the degree and rate of BBB passage, the *in vitro* model is able to predict passive or active transport of molecules, suggesting for example the involvement of efflux transporters.

Even though PET cannot describe BBB passage with such accuracy, the correlation between the *in vitro* and the *in vivo* pharmacokinetic data demonstrates that imaging reliably predicted the BBB passage for this series of derivatives of the radiopharmaceutical [^{18}F]F-A-85380. If such a strong agreement between the *in vitro* and *in vivo* pharmacokinetic data can be confirmed with other classes of molecules with different hydrophobic and molecular size ranges, the PET imaging method described here should prove useful for the rapid evaluation of the brain penetration of drug candidates.

ACKOWLEDGEMENTS

We are grateful to the staff of the instrumentation group at the SHFJ (Renaud Maroy, Vincent Brulon, Régine Trébossen).

REFERENCES

Audus KL and Borchardt RT (1986) Characteristics of the large neutral amino acid transport system of bovine brain microvessel endothelial cell monolayers. *J Neurochem.* **47**:484-488.

Begley DJ, Lechardeur D, Chen ZD, Rollinson C, Bardoul M, Roux F, Scherman D and Abbott NJ (1996) Functional expression of P-glycoprotein in an immortalised cell line of rat brain endothelial cells, RBE4. *J Neurochem.* **67**:988-995.

Bendayan R, Lee G and Bendayan M (2002) Functional expression and localization of P-glycoprotein at the blood brain barrier. *Microsc. Res. Tech* **57**:365–380.

Bottlaender M, Valette H, Roumenov D, Dolle F, Coulon C, Ottaviani M, Hinnen F and Ricard M (2003) Biodistribution and radiation dosimetry of 18F-fluoro-A-85380 in healthy volunteers. *J Nucl Med.* **44**:596-601.

Crone C (1963) The permeability of capillaries in various organs as determined by use of the indicator diffusion method. *Acta Physiol Scand.* **58**:292-305.

Davies B and Morris T (1993) Physiological parameters in laboratory animals and humans. *Pharm Res* **10**:1093-1095.

Dehouck MP, Jolliet-Riant P, Bree F, Fruchart JC, Cecchelli R and Tillement JP (1992) Drug transfer across the blood-brain barrier: correlation between in vitro and in vivo models. *J Neurochem.* **58**:1790-1797.

Deli MA and Joo F (1996) Cultured vascular endothelial cells of the brain. *Keio J Med* **45**:183-198.

Dishino DD, Welch MJ, Kilbourn MR and Raichle ME (1983) Relationship between lipophilicity and brain extraction of C-11-labeled radiopharmaceuticals. *J Nucl Med.* **24**:1030-1038.

Dollé F, Valette H, Bottlaender M, Hinnen F, Vaufrey F, Guenther I and Crouzel C (1998) Synthesis of 2-[^{18}F]fluoro-3-[2(S)-2-azetidinylmethoxy]pyridine, a highly potent radioligand for *in vivo* imaging central nicotinic acetylcholine receptors. *J Label Compds Radiopharm*, 41:451-463.

Dollé F, Dolci L, Valette H, Hinnen F, Vaufrey F, Guenther I, Fuseau C, Coulon C, Bottlaender M and Crouzel C (1999) Synthesis and nicotinic acetylcholine receptor in vivo binding properties of 2-fluoro-3-[2(S)-2-azetidinylmethoxy]pyridine: a new positron emission tomography ligand for nicotinic receptors. *J Med Chem.* **42**:2251-2259.

el-Bacha RS and Minn A (1999) Drug metabolizing enzymes in cerebrovascular endothelial cells afford a metabolic protection to the brain. *Cell Mol Biol* **45**:15-23.

Elmquist WF and Sawchuk RJ (1997) Application of microdialysis in pharmacokinetic studies. *Pharm Res*. **14:**267-288.

Franke H, Galla HJ and Beuckmann CT (1999) An improved low-permeability in vitro-model of the blood-brain barrier: transport studies on retinoids, sucrose, haloperidol, caffeine and mannitol. *Brain Res.* **818**:65-71.

Friebe M, Suda K, Spies H, Syhre R, Berger R, Johannsen B, Chiotellis E, Kramer SD and Wunderli-Allenspach H (2000) Permeation studies in vitro and in vivo of potential radiopharmaceuticals with affinity to neuro receptors. *Pharm Res*. **17**:754-760.

Gaillard PJ, Voorwinden LH, Nielsen JL, Ivanov A, Atsumi R, Engman H, Ringbom C, de Boer AG and Breimer DD (2001) Establishment and functional characterization of an in vitro model of the blood-brain barrier, comprising a co-culture of brain capillary endothelial cells and astrocytes. *Eur J Pharm Sci* **12**:215-222.

Gupta N, Price PM and Aboagye EO (2002) PET for in vivo pharmacokinetic and pharmacodynamic measurements. *Eur J Cancer*. **38**:2094-2107.

Hendrikse NH, Bart J, de Vries EG, Groen HJ, van der Graaf WT and Vaalburg W (2001) P-glycoprotein at the blood-brain barrier and analysis of drug transport with positron-emission tomography. *J Clin Pharmacol.* Suppl:48S-54S.

Huai-Yun H, Secrest DT, Mark KS, Carney D, Brandquist C, Elmquist WF and Miller DW (1998) Expression of multidrug resistance-associated protein (MRP) in brain microvessel endothelial cells. *Biochem Biophys Res Commun.* **243**:816-820.

Hughes CC and Lantos PL (1989) Uptake of leucine and alanine by cultured cerebral capillary endothelial cells. *Brain Res.* **480**:126-132.

Jeliazkova-Mecheva VV and Bobilya DJ (2003) A porcine astrocyte/endothelial cell co-culture model of the blood-brain barrier. *Brain Res Protoc.* **12**:91-98.

Kakee A, Terasaki T and Sugiyama Y (1996) Brain efflux index as a novel method of analyzing efflux transport at the blood-brain barrier. *J Pharmacol Exp Ther*. **277**:1550-1559.

Kimes AS, Horti AG, London ED, Chefer SI, Contoreggi C, Ernst M, Friello P, Koren AO, Kurian V, Matochik JA, Pavlova O, Vaupel DB and Mukhin AG (2003) 2-[18F]F-A-85380: PET imaging of brain nicotinic acetylcholine receptors and whole body distribution in humans. *FASEB J.* **17**:1331-1333.

Koeppe RA, Mangner T, Betz AL, Shulkin BL, Allen R, Kollros P, Kuhl DE and Agranoff BW (1990) Use of [11C]aminocyclohexanecarboxylate for the measurement of amino acid uptake and distribution volume in human brain. *J Cereb Blood Flow Metab.* **10**:727-739.

Laruelle M, Slifstein M and Huang Y (2003) Relationships between radiotracer properties and image quality in molecular imaging of the brain with positron emission tomography. *Mol Imaging Biol.* **5**:363-375.

Lundquist S, Renftel M, Brillault J, Fenart L, Cecchelli R and Dehouck MP (2002) Prediction of drug transport through the blood-brain barrier in vivo: a comparison between two in vitro cell models. *Pharm Res.* **19**:976-981.

Megard I, Garrigues A, Orlowski S, Jorajuria S, Clayette P, Ezan E and Mabondzo A (2002) A co-culture-based model of human blood-brain barrier: application to active transport of indinavir and in vivo-in vitro correlation. *Brain Res.* **927**:153-167.

Oldendorf WH (1970) Measurement of brain uptake of radiolabeled substances using a tritiated water internal standard. *Brain Res.* **24**:372-376.

Pardridge WM, Triguero D, Yang J and Cancilla PA (1990) Comparison of in vitro and in vivo models of drug transcytosis through the blood-brain barrier. *J Pharmacol Exp Ther.* **253**:884-891.

Parkinson FE, Friesen J, Krizanac-Bengez L and Janigro D (2003) Use of a three-dimensional in vitro model of the rat blood-brain barrier to assay nucleoside efflux from brain. *Brain Res.* **980**:233-241.

Pirro JP, Di Rocco RJ, Narra RK and Nunn AD (1994) Relationship between in vitro transendothelial permeability and in vivo single-pass brain extraction. *J Nucl Med.* **35**:1514-1519.

Rubin LL, Hall DE, Porter S, Barbu K, Cannon C, Horner HC, Janatpour M, Liaw CW, Manning K, Morales J et al (1991) A cell culture model of the blood-brain barrier. *J Cell Biol.* **115**:1725-1735.

Schellens JH, Malingre MM, Kruijtzer CM, Bardelmeijer HA, van Tellingen O, Schinkel AH and Beijnen JH (2000) Modulation of oral bioavailability of anticancer drugs: from mouse to man. *Eur J Pharm Sci* **12**:103-110.

Schinkel AH, Smit JJ, van Tellingen O, Beijnen JH, Wagenaar E, van Deemter L, Mol CA, van der Valk MA, Robanus-Maandag EC, te Riele HP et al (1994) Disruption of the mouse mdr1a P-glycoprotein gene leads to a deficiency in the blood-brain barrier and to increased sensitivity to drugs. *Cell.* **77**:491-502.

Takasato Y, Rapoport SI and Smith QR (1984) An in situ brain perfusion technique to study cerebrovascular transport in the rat. *Am J Physiol.* **247**:484-493.

Tanaka H and Mizojiri K (1999) Drug-protein binding and blood-brain barrier permeability. *J Pharmacol Exp Ther*. **288**:912-918.

Valette H, Bottlaender M, Dolle F, Guenther I, Fuseau C, Coulon C, Ottaviani M and Crouzel C (1999) Imaging central nicotinic acetylcholine receptors in baboons with [18F]fluoro-A-85380. *J Nucl Med.* **40**:1374-1380.

Van Bree JB, de Boer AG, Danhof M, Ginsel LA and Breimer DD (1988) Characterization of an "in vitro" blood-brain barrier: effects of molecular size and lipophilicity on cerebrovascular endothelial transport rates of drugs. *J Pharmacol Exp Ther.* **247**:1233-1239.

Weber SJ, Abbruscato TJ, Brownson EA, Lipkowski AW, Polt R, Misicka A, Haaseth RC, Bartosz H, Hruby VJ and Davis TP (1993) Assessment of an in vitro blood-brain barrier

model using several [Met5]enkephalin opioid analogs. *J Pharmacol Exp Ther*. **266**:1649-1655.

Wiesel FA, Blomqvist G, Halldin C, Sjogren I, Bjerkenstedt L, Venizelos N and Hagenfeldt L (1991) The transport of tyrosine into the human brain as determined with L-[1-11C]tyrosine and PET. *J Nucl Med.* **32**:2043-2049.

Wong DF and Pomper MG (2003) Predicting the success of a radiopharmaceutical for in vivo imaging of central nervous system neuroreceptor systems. *Mol Imaging Biol*. **5**:350-362.

FOOTNOTES

This study was supported in part by grants from the European FP5 OLIM program (contract QLG1-CT-2000-00562) the *Imagerie du petit animal* (IPA) CNRS-CEA program and the French National Agency for AIDS Research.

JPET Fast Forward. Published on October 6, 2005 as DOI: 10.1124/jpet.105.089102
This article has not been copyedited and formatted. The final version may differ from this version.

LEGENDS FOR FIGURES

Figure 1: Chemical structures of 10 selected *N*-substituted-azetidinyl and -pyrrolidinyl closely-related [^{18}F]fluoropyridinyl derivatives.

Figure 2 : Two compartment-model. k1 is the influx rate constant expressed in milliliter of blood per cubic centimeter of tissue per minute (mL.cm^{-3}.min^{-1}), k2 the efflux rate constant (min^{-1}), Cb(t) the concentration of radioactivity in the brain and Ca(t) the arterial input function.

Figure 3 : Fluorescence photomicrographs :

(A) Primary human astrocytes stained for GFAP (secondary antibody anti-mouse IgG, FITC-labelled). Nuclear staining with DAPI (blue). Scale bar = 25 µm.

(B) Unconfluent human brain microvascular endothelial cell component of the co-culture BBB model stained with the fluorescent probe DiI-acyl-LDL (red). This fluorescent marker accumulates around endothelial cells nuclei. Nuclear staining with DAPI (blue). Scale bar = 40 µm.

(C) Confluent human brain microvascular endothelial cells stained for CD31. Stack size: X:460.7 µm; Y: 460.7 µm

(D) Confluent BECs monolayer grown on filters and stained for tight junction protein claudin-1 (secondary antibody anti-mouse IgG, Alexa fluor 488-labelled). Stack size: X: 230.3 µm; Y: 230.3 µm

Figure 4 : Whole body PET images acquired over 2 min after the intravenous injection of the [^{18}F]fluoropyridinyl derivatives (upper panel, from left to right: [^{18}F]F-A-85380, [^{18}F]FPy 01,

02, 03, middle panel, from left to right: [^{18}F]FPy 04, 05, 06, 07, lower panel, from left to right: [^{18}F]FPy 08, 09, 10).

Figure 5: *In vivo* early cerebral kinetics derived from the volumes of interest (VOI) drawn on the cerebral area on the PET images. All radioactivity concentrations are the mean of four experiments and are expressed as a percentage of the injected dose per volume of tissue (%ID.cm^{-3}). Standard deviations ranged from 0.01 to 0.18 %ID.cm^{-3} (not shown).

Figure 6: Whole blood kinetics. In order to estimate the input function, two animals were injected for arterial blood sampling and radioactivity counting. All values are the mean of two experiments and are expressed as a percentage of injected dose per volume of blood (%ID.mL^{-1}). Standard deviations ranged from 0.01 to 0. 26 %ID.mL (not shown).

Figure 7: Comparison of the *in vitro* PSe-out/PSe-in ratio (Q ratio) and the *in vivo* distribution volume (DV).

Figure 8: *In vitro/in vivo* correlation: *in vivo* permeability coefficient (PS) as a function of the *in vitro* permeability coefficient (PSe-in).

JPET Fast Forward. Published on October 6, 2005 as DOI: 10.1124/jpet.105.089102
This article has not been copyedited and formatted. The final version may differ from this version.

Table 1: Molecular weights, octanol/Phosphate buffer saline (pH 7.4) partition coefficients (log D), *in vitro* permeability coefficients (PSe-in and PSe-out) and PSe-out/PSe-in ratios (Q ratio) measured with the *in vitro* human BBB model for the 11 compounds studied.

Derivatives	**MW** ($g.mol^{-1}$)	**Log D** (pH 7.4)	**PSe-in** ($\mu L.min^{-1}$)	**PSe-out** ($\mu L.min^{-1}$)	**Q ratio**
F-A-85380	182.2	-1.49	5.68	4.48	0.9
FPy 01	317.4	1.23	10.39	6.46	0.6
FPy 02	281.3	0.63	10.04	36.85	3.7
FPy 03	286.3	1.93	59.42	34.26	0.6
FPy 04	266.3	1.57	12.87	51.38	4.0
FPy 05	585.6	1.36	3.34	8.12	2.4
FPy 06	321.4	1.95	6.47	24.87	3.8
FPy 07	337.5	1.15	19.58	5.43	0.3
FPy 08	300.3	1.74	16.22	12.66	0.8
FPy 09	315.3	1.76	8.70	3.91	0.5
FPy 10	295.4	1.74	1.68	3.67	2.2

JPET Fast Forward. Published on October 6, 2005 as DOI: 10.1124/jpet.105.089102
This article has not been copyedited and formatted. The final version may differ from this version.

Table 2: *In vivo* influx rate constants (k1), efflux rate constants (k2), distribution volumes (DV) and permeability coefficients (PS) for the 11 compounds studied. Variation coefficients are mentioned in parentheses.

Derivatives	**k1** ($mL.cm^{-3}.min^{-1}$)	**k2** (min^{-1})	**DV** ($mL.cm^{-3}$)	**PS** ($mL.min^{-1}.cm^{-3}$)
F-A-85380	0.10 (2.4%)	0.04 (4%)	2.33	0.10
FPy 01	0.66 (3.4%)	0.87 (3.9%)	0.76	0.79
FPy 02	0.32 (3.3%)	1.12 (0.6%)	0.28	0.35
FPy 03	2.00 (4.9%)	2.08 (2.5%)	0.96	6.39
FPy 04	0.65 (10.5%)	1.43 (11.1%)	0.45	0.78
FPy 05	0.15 (3.6%)	0.84 (0.9%)	0.17	0.16
FPy 06	0.29 (2.3%)	0.98 (1.4%)	0.29	0.31
FPy 07	1.07 (3.6%)	1.22 (1.0%)	0.88	1.50
FPy 08	1.03 (8.7%)	1.24 (4.4%)	0.83	1.42
FPy 09	0.34 (7.1%)	0.40 (2.5%)	0.85	0.37
FPy 10	0.15 (9.4%)	0.30 (10.4%)	0.48	0.15

JPET Fast Forward. Published on October 6, 2005 as DOI: 10.1124/jpet.105.089102
This article has not been copyedited and formatted. The final version may differ from this version.

Figure 1

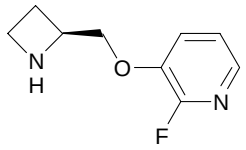

F-A-85380

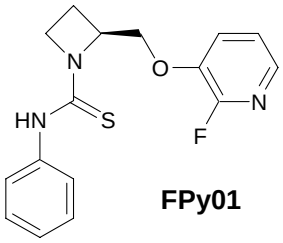

FPy01

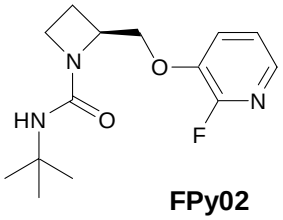

FPy02

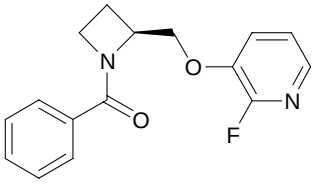

FPy03

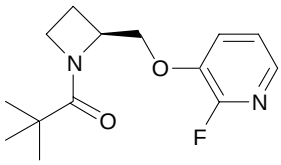

FPy04

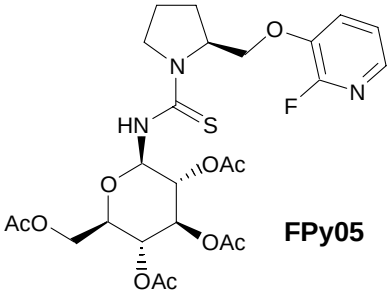

FPy05

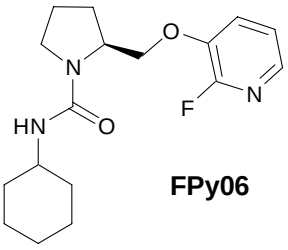

FPy06

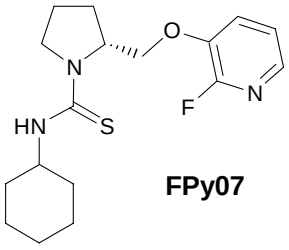

FPy07

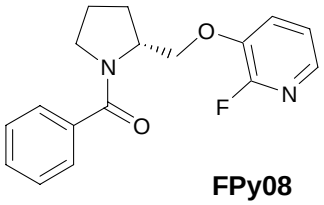

FPy08

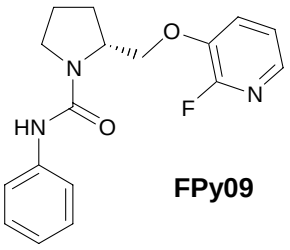

FPy09

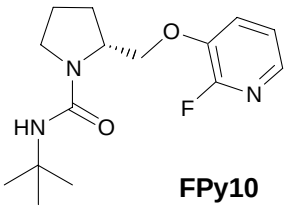

FPy10

JPET Fast Forward. Published on October 6, 2005 as DOI: 10.1124/jpet.105.089102
This article has not been copyedited and formatted. The final version may differ from this version.

Figure 2

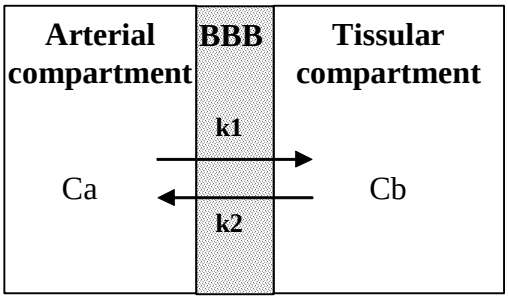

Figure 3

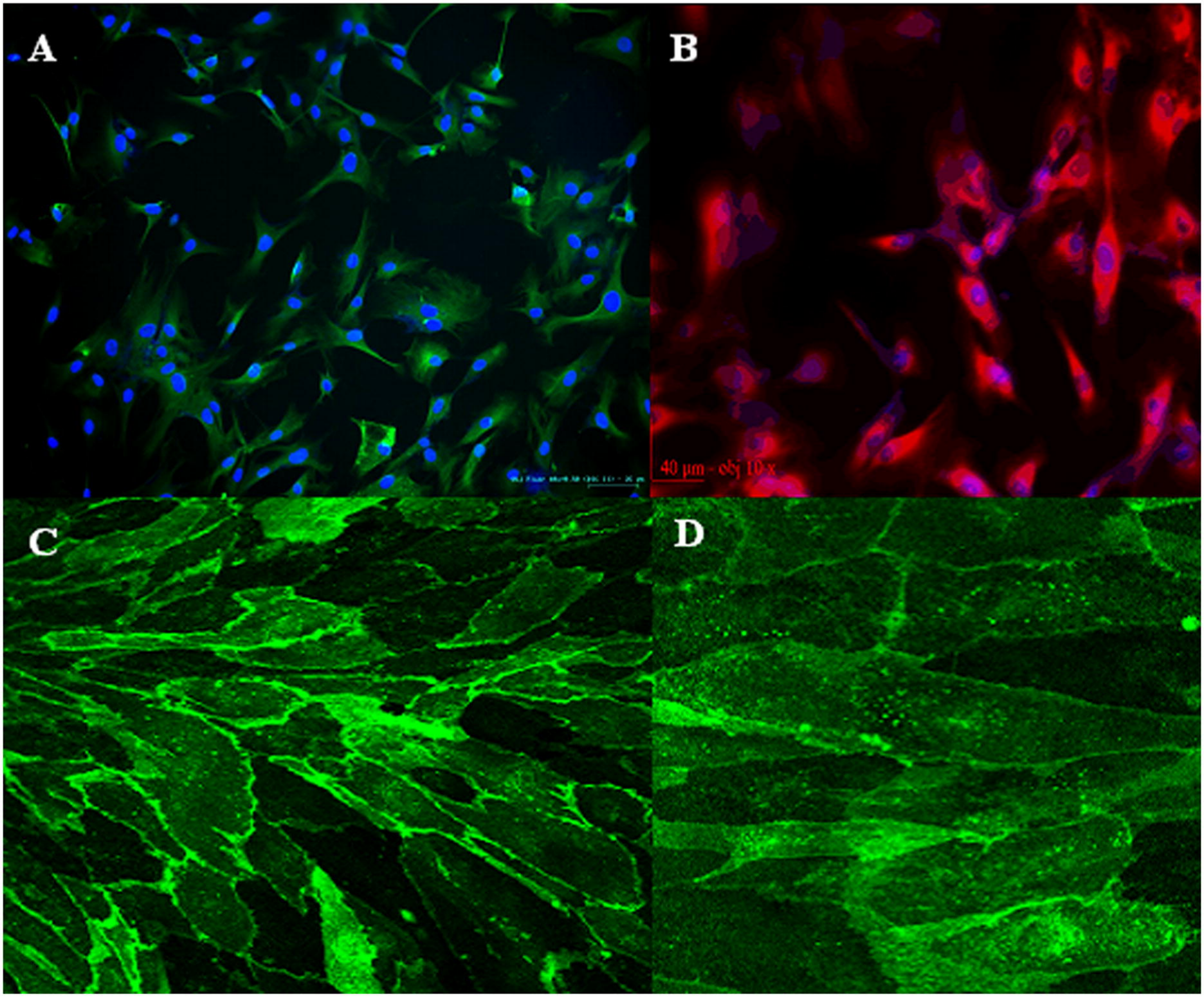

Figure 4

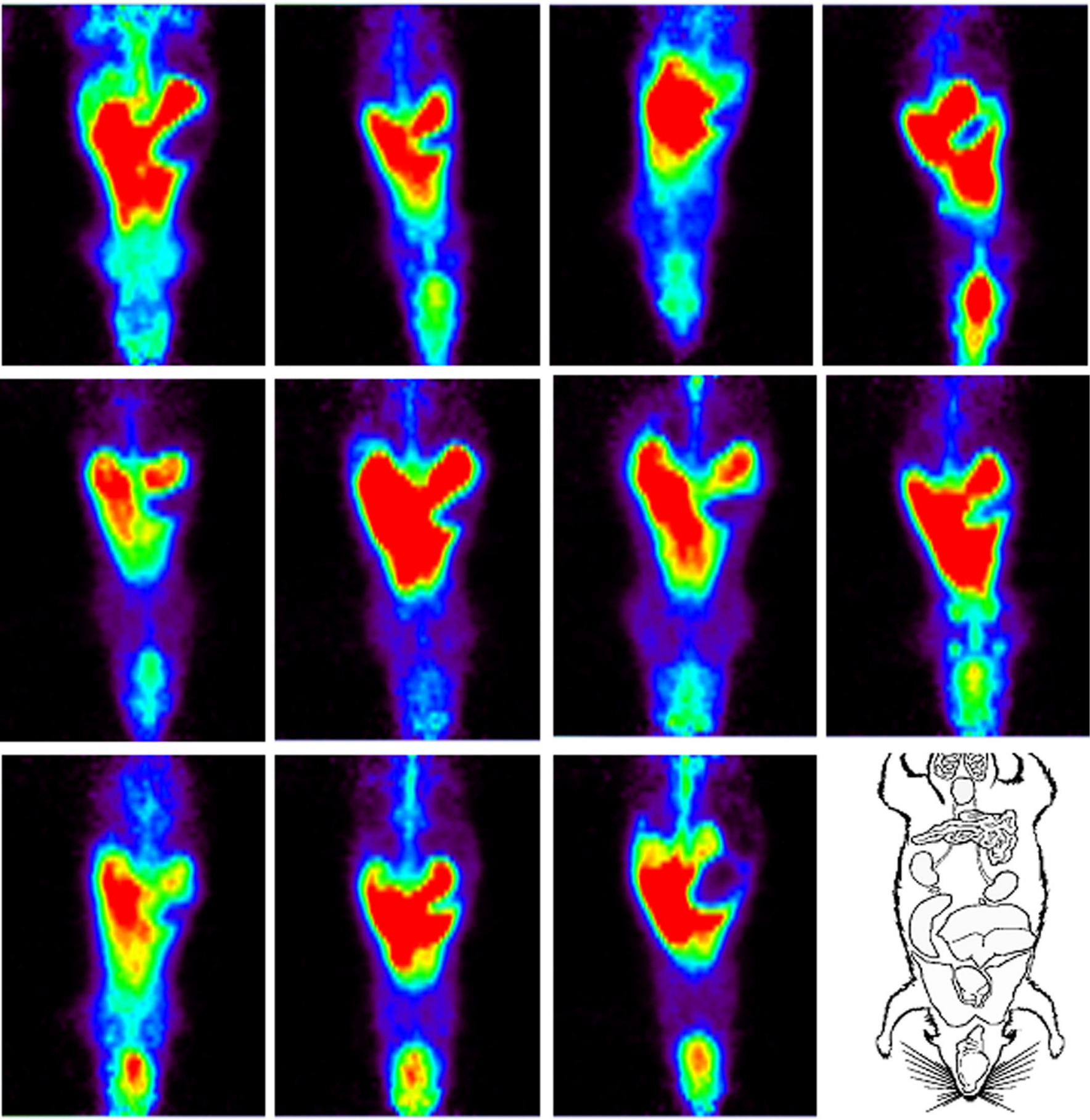

JPET Fast Forward. Published on October 6, 2005 as DOI: 10.1124/jpet.105.089102
This article has not been copyedited and formatted. The final version may differ from this version.

Figure 5

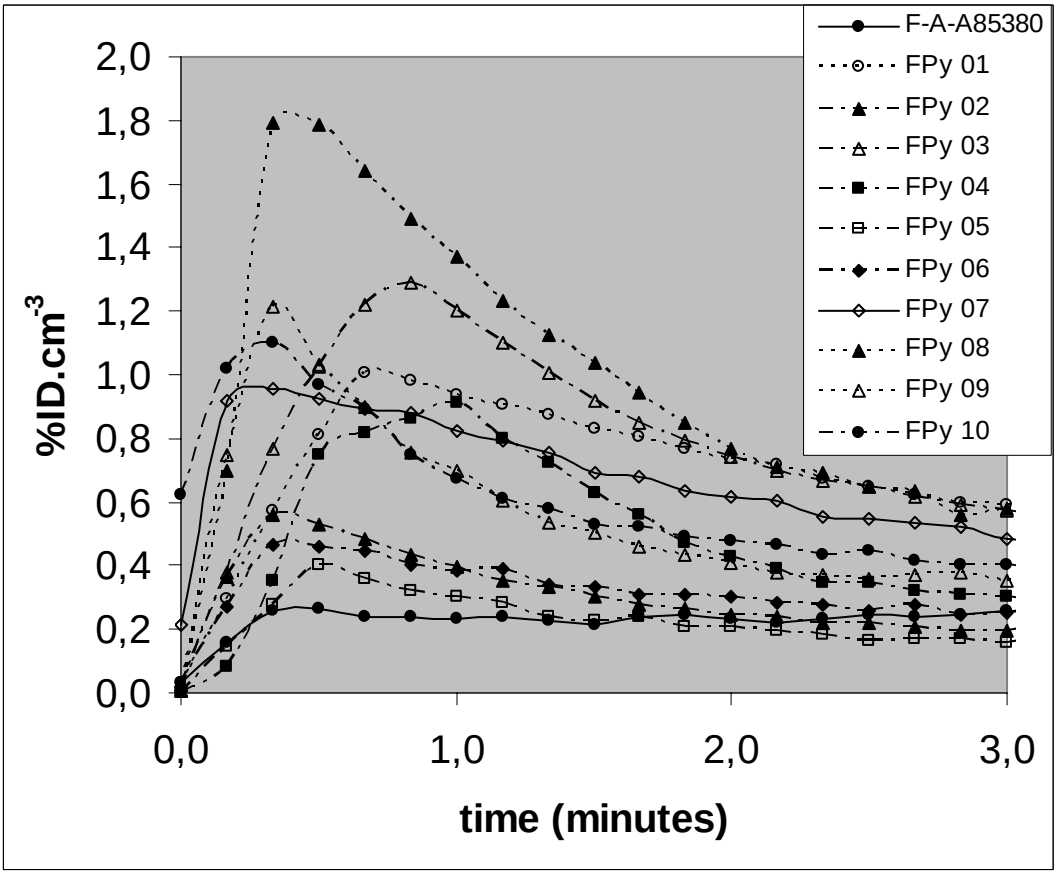

JPET Fast Forward. Published on October 6, 2005 as DOI: 10.1124/jpet.105.089102
This article has not been copyedited and formatted. The final version may differ from this version.

Figure 6

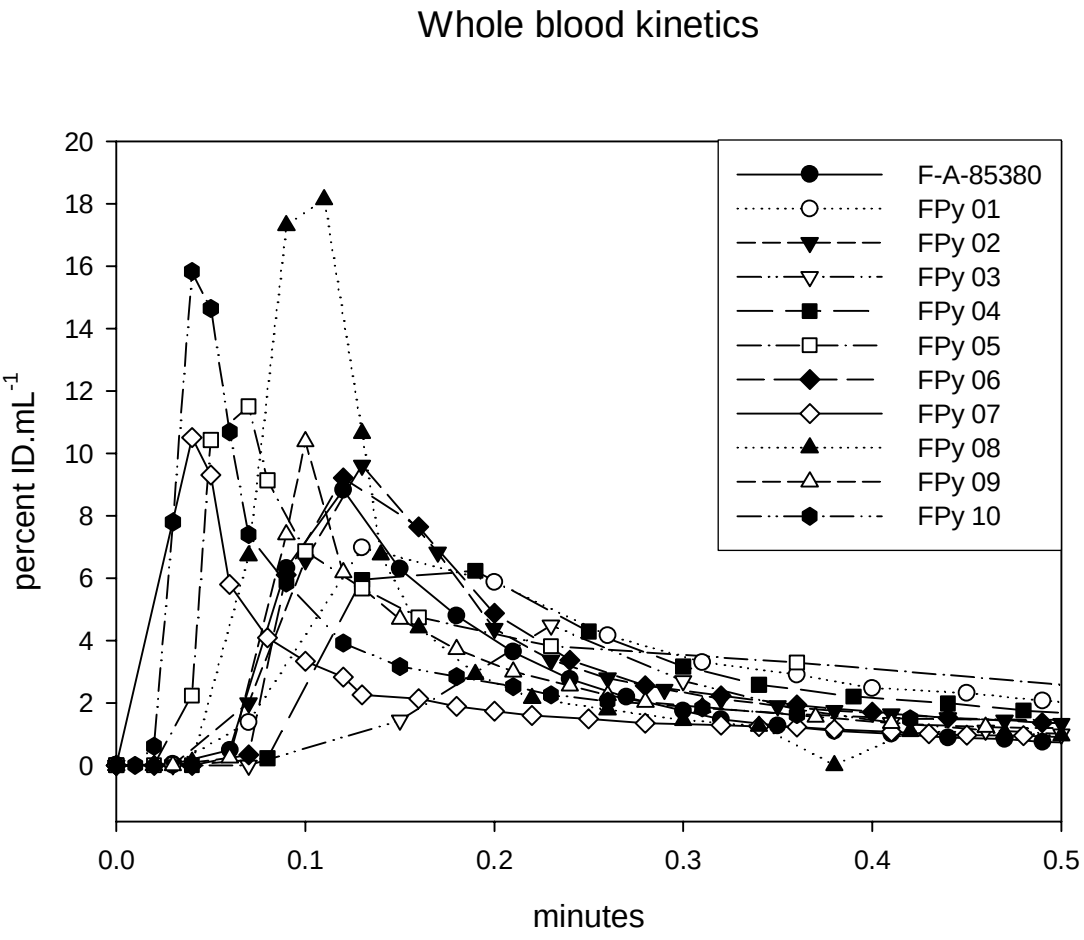

JPET Fast Forward. Published on October 6, 2005 as DOI: 10.1124/jpet.105.089102
This article has not been copyedited and formatted. The final version may differ from this version.

Figure 7

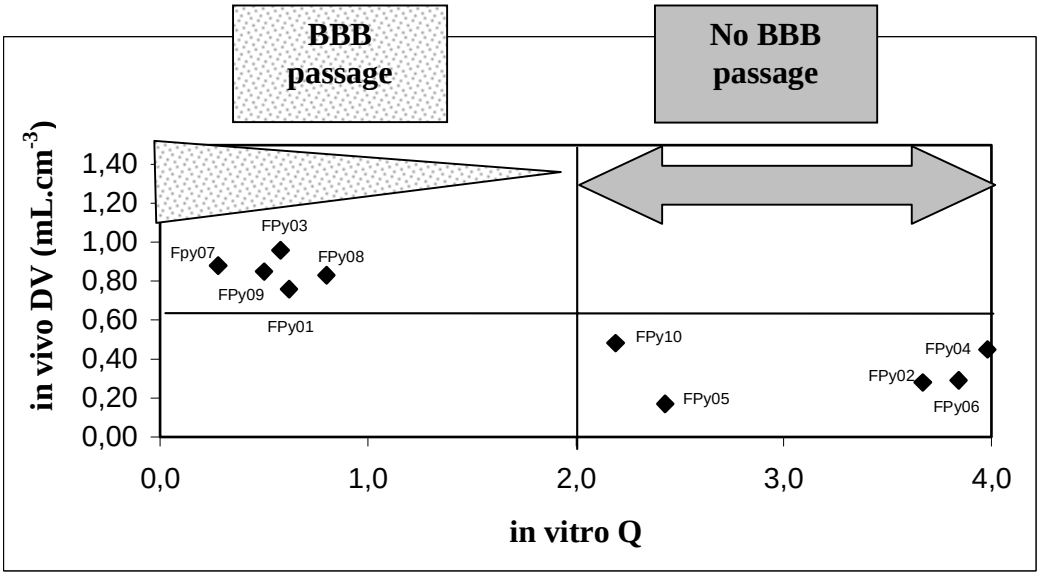

JPET Fast Forward. Published on October 6, 2005 as DOI: 10.1124/jpet.105.089102
This article has not been copyedited and formatted. The final version may differ from this version.

Figure 8